

# Shear-thickening and shear-induced pattern formation in starch solutions<sup>☆</sup>

S. Kim\*, J.L. Willett, C.J. Carriere, F.C. Felker

National Center for Agricultural Utilization Research, Agricultural Research Service, USDA, 1815 N. University Street, Peoria, IL 61614, USA

Received 27 September 2000; revised 26 January 2001; accepted 26 January 2001

## Abstract

Since Dintzis et al. reported shear-thickening behavior and shear-induced pattern formation in semidilute starch solutions for the first time in 1995, considerable efforts have been made to understand the science behind these observations. Despite these efforts, however, many questions regarding this behavior of starch solutions remain. Using a Brookfield programmable rheometer and a custom-built shear microscope, starch solutions in alkaline solution medium were investigated. In this report, we present data leading to the following conclusions: (1) gently prepared starch solutions are macroscopically heterogeneous with regions of highly concentrated gel-like structures dispersed in dilute starch solution; (2) shear breaks up these heterogeneous regions, increasing in viscosity (shear-thickening) which is thus seen to be a result of an increase in the concentration of dissolved starch; (3) pattern formation, observed when the solution is exposed to higher shear rate, is the result of a separate shear-induced aggregation process; and (4) aggregations are not induced below a certain critical threshold shear rate and time is also a factor in the behavior of the aggregate. Published by Elsevier Science Ltd.

**Keywords:** Starch solutions; Shear-thickening; Shear-induced pattern formation; Shear-induced aggregation; Shear microscopy

## 1. Introduction

Some years ago, shear-thickening and quasi-hysteresis loops of shear stress versus strain rate in waxy maize starch solutions were reported for the first time (Dintzis & Bagley, 1995). The behavior of waxy maize starch in dimethyl sulfoxide was observed to be similar to that in aqueous base. In the subsequent report (Dintzis, Bagley & Felker, 1995), the authors added another observation; shear-induced structure formation occurred in the sheared waxy maize starch solutions. Since its texture was visible only with a phase-contrast microscope, the formed pattern was an indication of refractive index inhomogeneities in the fluids. In the third report (Dintzis, Berhow, Bagley, Wu & Felker, 1996), various starches, i.e. waxy maize, waxy rice, waxy barley, potato, cassava, normal rice, wheat, and normal maize were examined to verify shear-thickening behavior. As a result, they concluded that gently treated 2–3% starch solutions (waxy maize, waxy rice, waxy barley, and potato) in 90% DMSO or 0.2 N NaOH show shear-thickening behavior to a greater extent than did wheat, normal rice, or normal maize starches. From these experiments, shear-thickening was

found to be general for waxy starch solutions. It was also clearly shown that amylopectin is responsible for shear-thickening by comparing shear viscosities of fractionated amylose and amylopectin. In the same report, it was stated that even non-waxy starches exhibit some degree of shear-thickening in 0.2 N NaOH solution. They concluded that shear-thickening is a reflection of the structure forming process by amylopectin and as a result of this process shear-induced structures are observed in starch solutions. Both phase-contrast micrographs and circular dichroism data obtained from starch solutions with and without shearing were used as supporting evidences for this conclusion. In this report, however, we will be showing that this conclusion is not a complete description of the phenomenon.

We focused our efforts on the following issues: (1) What is the relationship between shear-thickening and pattern formation? (2) What causes shear-thickening behavior? (3) Why is gentle preparation required for shear-thickening? (4) Why is shear-thickening irreversible? (5) What is the entity of the formed pattern in the sheared solution?

## 2. Materials and methods

### 2.1. Materials

A waxy maize starch (WM), designated as Amioca, consisting of about 98% amylopectin was obtained from

<sup>☆</sup> Names are necessary to report factually on available data; however, the USDA neither guarantees nor warrants the standard of the product, and the use of the name by the USDA implies no approval of the product to the exclusion of others that may also be suitable.

\* Corresponding author.

American Maize Products Company (Hammond, IN). A normal maize (NM, cat# S4126) starch was purchased from Sigma Chemical Co. Normal maize is unmodified regular starch containing approximately 73% amylopectin and 27% amylose. All the starches were used as received. All other chemicals used were reagent grade.

## 2.2. Solution preparation

The stirred starch in NaOH solutions were prepared by the procedure used in a previous report (Dintzis et al., 1995). The procedure is as follows: the starch was first mixed thoroughly with 2 ml of distilled water to dampen all granules; then 20 ml of 1 N NaOH was added to the mixture and stirred vigorously with a spatula for 10–20 min to disrupt all granules and dissolve them. Distilled water was slowly added to the starch with stirring to achieve a uniform solution in 0.2 N NaOH.

## 2.3. Programmable rheometer

Rheological properties were measured with a Brookfield Programmable Rheometer (Model DV-III) equipped with a coaxial cylinder cell. The shear field was applied as a step by step format with custom software written with QBASIC. Typical dwell time at a given shear rate was 5 s with shear-rate range of 1–230 s<sup>-1</sup>. By rewriting the controlling software, the shear-rate range and the dwell time at particular shear rates could be modified arbitrarily. All the measurements were performed at 23.0 ± 0.1°C.

## 2.4. Shear microscopy

A microscope system was constructed for use in taking images of sheared starch solutions. A schematic diagram of the instrument is shown in Fig. 1. The shear cell was

composed of a cone and plate geometry made of quartz. The diameter and cone angle of the cone were 44 mm and 1.5°, respectively. The shear rate was controlled by a computer terminal, which serially interfaced the motor. The instrument is equipped with a phase-contrast microscope.

The microscopic images were collected by a CCD camera (Dage MTI, model 72). The electronic shutter time of the CCD camera, 1/30 s/frame, is long enough to cause smeared images when it is used to monitor and capture the images of the moving objects in the microscope field. In order to avoid this problem, a custom-built flash was used. Since the CCD controller generates a pulse every 1/60 s, a custom-built timing circuit was used to reform this pulse to produce pulses every 1/30 s. This reformed pulse actuated the flash circuit to supply power voltage to the lamp. In this way, image smearing could be avoided. The duration of the flash light pulse was ca. 4 μs.

The desired image frames were digitized to the resolution of 640 × 480 pixels with a frame grabber and processed with a PC. The prototype of this instrument was described in an earlier publication (Kim, Yu & Han, 1996).

## 2.5. Optical microscopy

Sheared samples were observed with a Zeiss Axioskop microscope using a 10× objective and phase-contrast optics. Still images were recorded with a Kodak DCS460 digital camera at a resolution of 3060 × 2036.

## 3. Results and discussion

The typical shear-thickening behavior of 2% WM in 0.2 N NaOH solution is shown in Fig. 2. As the shear rate is increased, shear-thickening appears in the shear-rate

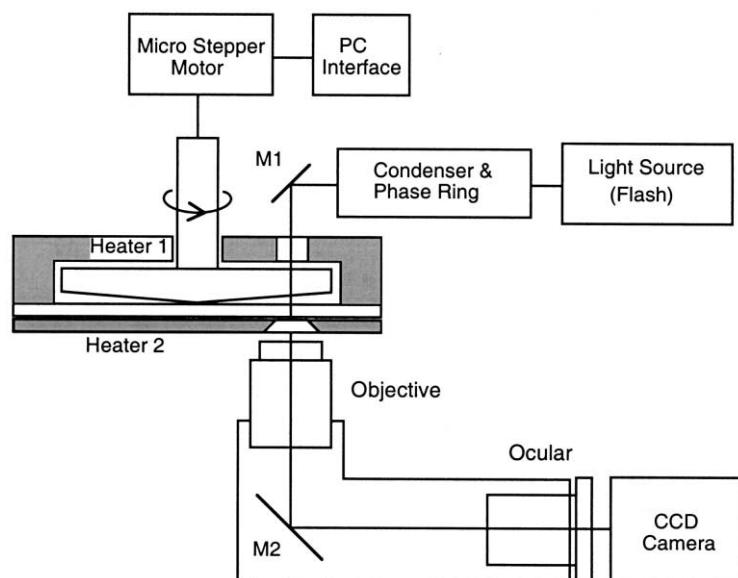


Fig. 1. Schematic diagram of shear-microscope.

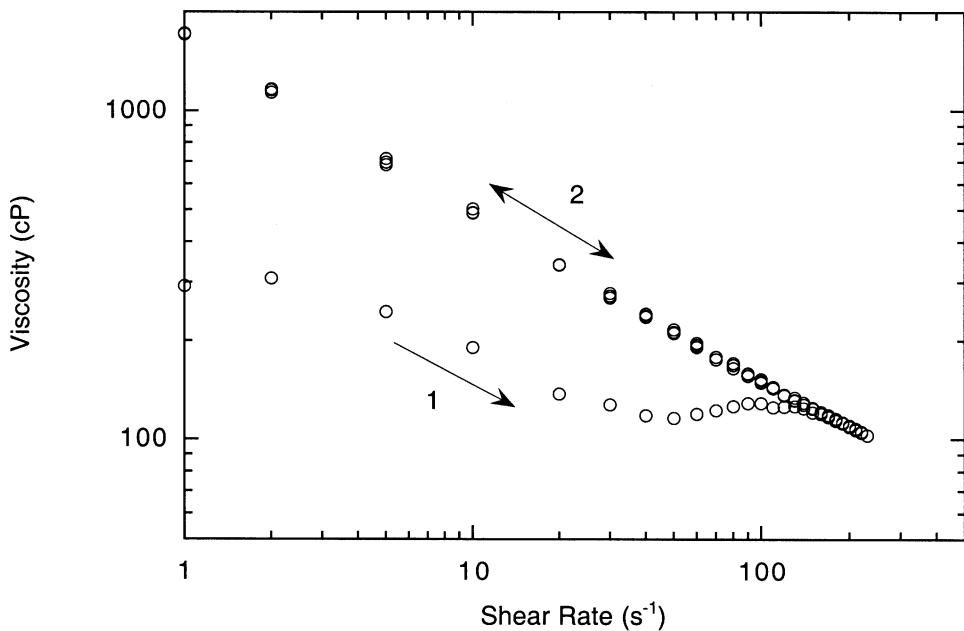


Fig. 2. Typical shear-thickening behavior of 2% WM in 0.2 N NaOH solution. The viscosity trend does not change after the first cycle of the measurement.

range of 50–100 s<sup>-1</sup> (curve #1 in Fig. 2). After the first cycle of the viscosity measurement, increasing or decreasing the shear rate did not show significant change in the viscosities (curve #2 in Fig. 2). In other words, only the first cycle from low to high shear rate displays shear-thickening. Although we show a typical shear-thickening behavior, this flow behavior was sensitive to sample preparation, sample treatment, time between sample preparation and measurement, etc., as was reported previously (Dintzis et al., 1996). Hence, exact replication of shear-dependent apparent viscosity, especially for the shear-thickening region, is not to be expected. The reason for these observations will be given in the concluding part of this report. Pattern formation was always observed after shear viscosity measurements whether or not the solution showed shear-thickening.

The first step for this research is to determine the relationship, if any, between the two phenomena, shear-thickening and pattern formation. The pattern formation has been observed only after shear-viscosity measurements. If pattern formation is a consequence of shear-thickening, pattern formation should be observed just after the sample solution experiences shear-thickening. To verify this assumption, the same solution used for Fig. 2 was examined with a microscope just after passing the shear-thickening region, i.e. when curve #1 in Fig. 2 reached 150 s<sup>-1</sup>. No pattern formation could be identified in the sample solution.

In the previous report (Dintzis et al., 1996), it was believed that the shear-thickening is a reflection of the structure forming process by amylopectin and as a result of this process shear-induced structures are observed in starch solutions. If this were the case, a severely treated solution, which does not show shear-thickening behavior and only displays shear-thinning behavior like curve #2 in Fig. 2, should

reveal pattern formation. The experimental result turned out to be negative. The patterns were observed only when the solution was sheared for an extended time period at higher than critical shear rate. Explicit experimental data are shown later in this report (Fig. 6).

From the above two experimental results, it is concluded that shear-thickening is not a prerequisite for the formation of patterns in the solution; they are two separate phenomena. Hence, the first question posed in Section 1 of this report is answered.

As a second step for this research, we tried to understand the nature of shear-thickening behavior. For that purpose, the software that controls the measurement process of shear viscosity was modified to change the scanning shear-rate range and dwell time at each shear rate. From a series of experiments at various conditions, it is found that the overall profile of shear viscosity changes significantly depending on the shear-rate range and dwell time at each shear rate. Evaluation of each set of data led us to conclude that shear-thickening is a reflection of a structure-breaking process. In other words, it seems that some structure in the solution is disrupted when the solution shows shear-thickening behavior. To verify this assumption, the software was modified to stay for an extended time, 60 s, at a certain shear rate while the dwell time at other shear rates were fixed at 5 s during the course of shear viscosity measurement. The experimental results are displayed in Fig. 3. According to these data, 20 s<sup>-1</sup> is not a strong enough shear field to break the structures in the sample material. The overall viscosity profile is not much affected by this modification. However, the rest of the data shows that 50 s<sup>-1</sup> and higher shear rates are high enough to break the structures. From these data, we can conclude that there is a

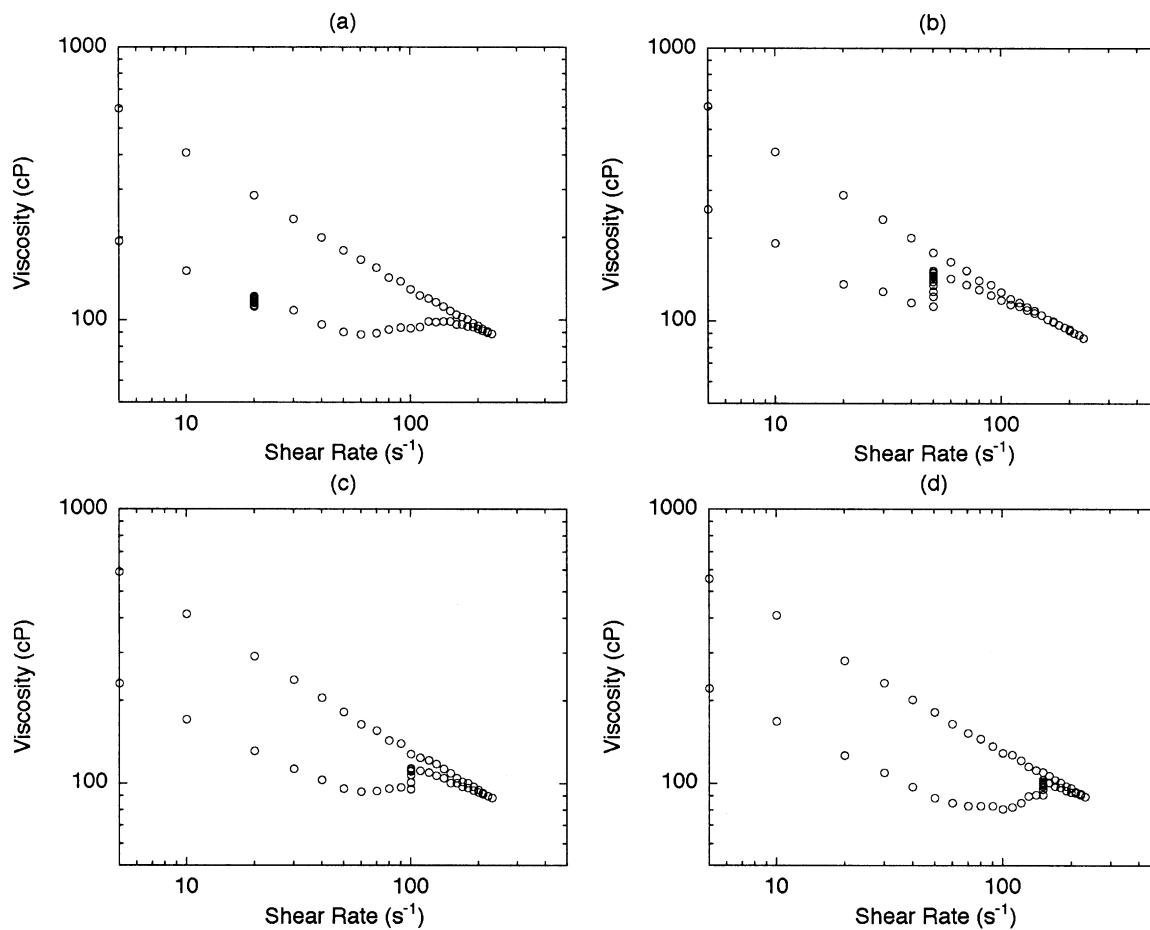


Fig. 3. Shear time dependence of apparent viscosity in the shear-thickening region. An extended period of time, 60 s, was allowed at certain shear rates during viscosity measurements: (a) at  $20\text{ s}^{-1}$ ; (b) at  $50\text{ s}^{-1}$ ; (c), at  $100\text{ s}^{-1}$ ; and (d) at  $150\text{ s}^{-1}$ . It is shown that higher than  $20\text{ s}^{-1}$  is required for breaking the “structures” effectively.

critical shear rate, in between  $20$  and  $50\text{ s}^{-1}$ , above which the structures are readily broken.

Further support for the above interpretation is provided by the next experiment. In Fig. 4, the shear rate scan is performed between  $1$  and  $50\text{ s}^{-1}$  for the first two cycles and  $1$  and  $230\text{ s}^{-1}$  for the next two cycles. Even when the maximum shear rate was limited to  $50\text{ s}^{-1}$ , a hysteresis in the viscosity loop was observed. It is noteworthy that the second half-cycle of the first scan mostly overlaps the first half-cycle of the second scan. The same trend is observed with the second half-cycle of the second scan and the first half-cycle of the third scan. It should be noted that shear rates between  $30$  and  $50\text{ s}^{-1}$  for the first two cycles contribute to the change in the viscosity profile. However, the shear is not intense enough in these two cycles to break the whole structures in the solution in a given time frame. In the case of the third and fourth cycle, it is clear that the structures in the solution are fully broken and the viscosity trend would not change any more.

In addition to the above two sets of data, other evidence relates shear-thickening to a structure-breaking process. When the solutions are prepared for the experiment, some

clusters were visually observed in the solution. The reason for the existence of clusters is as follows.

When the starch solutions are prepared by the procedures specified by Dintzis et al. (1996), an intermediate solution with higher than overlap concentration was prepared first and then dilution process was followed. Since the starch molecules in this highly concentrated solution are severely entangled, the dilution process does not yield a homogeneous solution immediately. Rather, a heterogeneous mixture of highly entangled clusters in a dilute starch solution is formed. Hence, it is appropriate to call this mixture a dispersion of clusters. In this situation, the measured viscosity of the solution does not have the same meaning as that of the homogeneous solution. When this dispersion of clusters is exposed to the shear field for the viscosity measurement, there are two sources that contribute to shear stresses at lower than critical shear rate — one from the solvent medium with low concentration of starch and the other from highly concentrated starch clusters. When shear fields are applied to the solution, the clusters roll between two shear cells contributing to shear stress to a small extent. As a result, the viscometer reports far lower viscosity than is

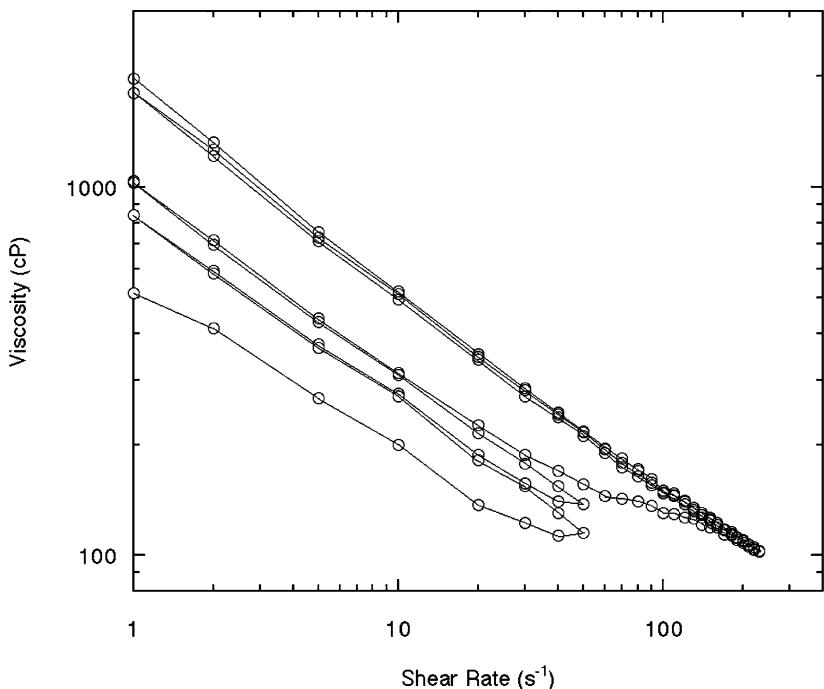


Fig. 4. Maximum shear rate was modified for each cycle of the viscosity measurement: the first and second cycle,  $50\text{ s}^{-1}$ ; the third and fourth cycle,  $230\text{ s}^{-1}$ . Once the solution experiences  $230\text{ s}^{-1}$ , the apparent viscosity does not change any more.

expected for a given homogeneous starch solution. As shear rate is increased to a certain threshold shear rate, the clusters begin to be disrupted resulting in higher overall concentration of the solution. As a result, the apparent viscosity of the solution increases during this time. That is why we observe shear-thickening behavior in the starch solutions. After the solution experiences shear-thickening, it becomes homogeneous.

The sizes of molecules in starch solutions are not expected to exceed  $5\text{ }\mu\text{m}$  according to previous reports (Fishman, Rodriguez & Chau, 1996; Millard, Wolf, Dintzis & Willett, 1999). However, a gently prepared dispersion could not pass through a  $5\text{-}\mu\text{m}$  filter. After a shear-thickening treatment, the solution passes through the filter. This is the direct evidence of the existence of clusters, larger than  $5\text{ }\mu\text{m}$ , in the initial solution. Since the size of some clusters is very large (on the order of a few millimeters), they could be identified with a laser beam (He–Ne laser, wavelength =  $632.8\text{ nm}$ ) by manually scanning the dispersion. The large difference in refractive indices between clusters and the dispersion medium enables us to identify the existence of clusters easily. These large domains can even be identified when the sample vial is illuminated with white light.

Shear-thickening was observed in dispersions only when the clusters were present. If the solution is prepared without inclusion of the dilution process, it does not show shear-thickening. The best condition for observing shear-thickening behavior is that the clusters are well dispersed in the dispersion medium with not-too-small sizes. Gentle

preparation is needed not to disrupt the clusters. Since the clusters get disrupted in the dispersion medium with time, the time interval between sample preparation and viscosity measurement is another important factor to observe shear-thickening.

Previously, it was reported that NM solution does not show shear-thickening while WM solution does (Dintzis & Bagley, 1995; Dintzis et al., 1995, 1996). According to the above interpretation, however, the starch does not have to be waxy maize to show shear-thickening behavior. As long as the starch forms gel-like clusters which are not readily disrupted in the solvent medium without shear field, shear-thickening behavior is expected. As an example, a shear-thickening behavior obtained with 1.5% normal maize in  $0.2\text{ N NaOH}$  solution is shown in Fig. 5. The reason why shear-thickening is not observed with NM is that it requires more careful preparation of the solution. When the sample vials were gently shaken, the clusters in WM solution were more resistant to disruption than those in NM solution. Hence, it is concluded that the clusters formed from NM are less stable than those from WM starches. That should be why the shear-thickening in NM starch solutions has not been reported yet. However, if the solutions are carefully prepared not to disrupt the clusters, a shear-thickening behavior can be clearly observed as in Fig. 5.

From these experimental results, it is concluded that the clusters, macroscopic heterogeneities, which have been formed during the sample preparation process, are broken and dispersed during the first viscosity measurement cycle and its breaking process is observed as shear-thickening. In

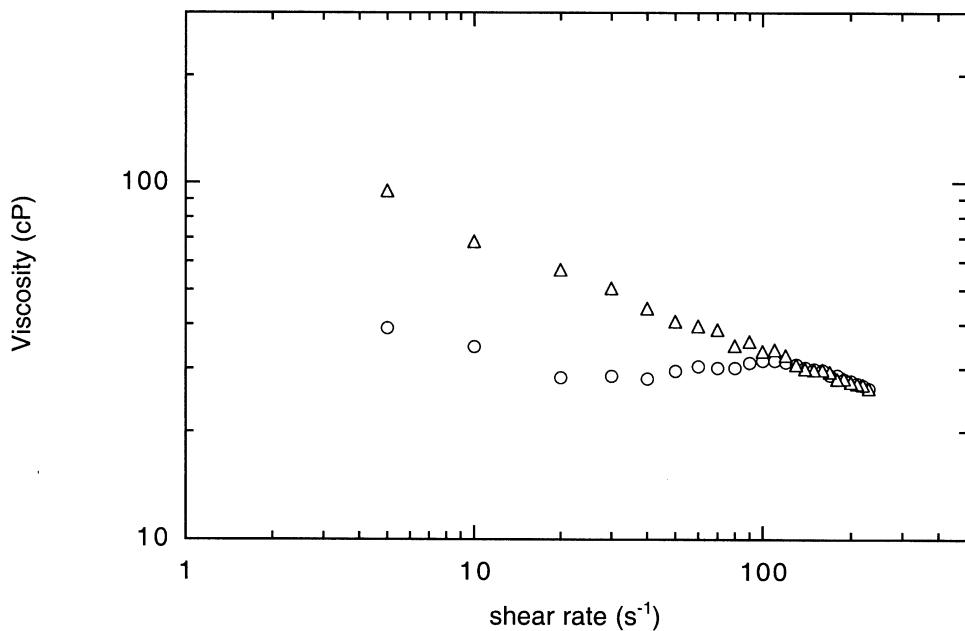


Fig. 5. Shear-thickening behavior of 1.5% NM in 0.2 N NaOH solution.

this way, the second, third and fourth questions posed in Section 1 of this report are answered. The above argument confirms that shear-thickening behavior and pattern formation are not related.

So far, we have focused on the gently prepared starch solutions to explain the reason for shear-thickening behavior reported previously. It can be argued that if we try not to form clusters during the sample preparation, we are not supposed to observe shear-thickening behavior. To verify this prediction, the sample preparation procedure was modified: For example, 200 mg of starch is first mixed thoroughly with 5 ml of distilled water to dampen all granules; then 5 ml of 1 N NaOH was added to the mixture while stirring the starch suspension. As soon as NaOH solution is added, the starch granules gelatinize in a few seconds, and eventually, the whole solution becomes clear. The starch solutions prepared in this way did not show an appreciable amount of clusters when inspected with a white light or Ne-He laser beam. The viscosity data from as-prepared solutions showed no shear-thickening behavior. Still, however, a small amount of hysteresis in the viscosity was observed. This result indicates the difficulty in the preparation of homogeneous starch solutions. These difficulties originate from the fact that the solubilization of starch entails gelatinization of granules. Also, the huge molecular weight of amylopectin is another factor whereby no solvents are effective enough to solubilize completely the starch granules in a short time.

Another possible explanation for the observed shear-thickening is the presence of blocklets (Gallant, Bouchet & Baldwin, 1997) in starch granules. The blocklets could survive during sample preparation, and be disrupted during application of high shear fields. If this is the case, however,

shear-thickening behavior should be observed whether or not the sample preparation procedure includes a dilution step. When the solutions do not show shear-thickening, the apparent viscosity data follows curve #2 only (Fig. 2). When the solutions show shear-thickening, both curve #1 and #2 are shown as in Fig. 2. The dependence of shear-thickening on sample preparation implies that the blocklet structures suggested by Gallant et al. are not the source of the observed shear-thickening.

The third step of the research is investigating the entity of patterns formed by the shear field. According to the previous reports (Dintzis et al., 1995, 1996), the images of shear-induced patterns were obtained after completion of the shear viscosity measurements. Hence, it is not known when during the shearing cycle the patterns were generated or what the best conditions for pattern generation are. In the case of semidilute solution of high molecular weight polystyrene, shear-induced phase separation had been reported earlier (Ver Strate & Phillipoff, 1974). Later, more investigations were performed on this issue by adopting shear light scattering and shear microscopy techniques (Hashimoto & Kume, 1992; Moses, Kume & Hashimoto, 1994). Considering the similarity of these two cases, i.e. involvement of high molecular weight polymer, semidilute solution, and shear-induced pattern formation, it is believed that a direct observation of the process under a microscope would help us to answer the unresolved questions. Such shear microscopy allowed us to observe the formed patterns in the solution during application of shear field. When the starch solutions were sheared with gradually increasing shear rates, it was found that the patterns were formed at high shear rates only (higher than  $100\text{ s}^{-1}$ ) and the extent of pattern formation increased as shear time was increased (Fig. 6).

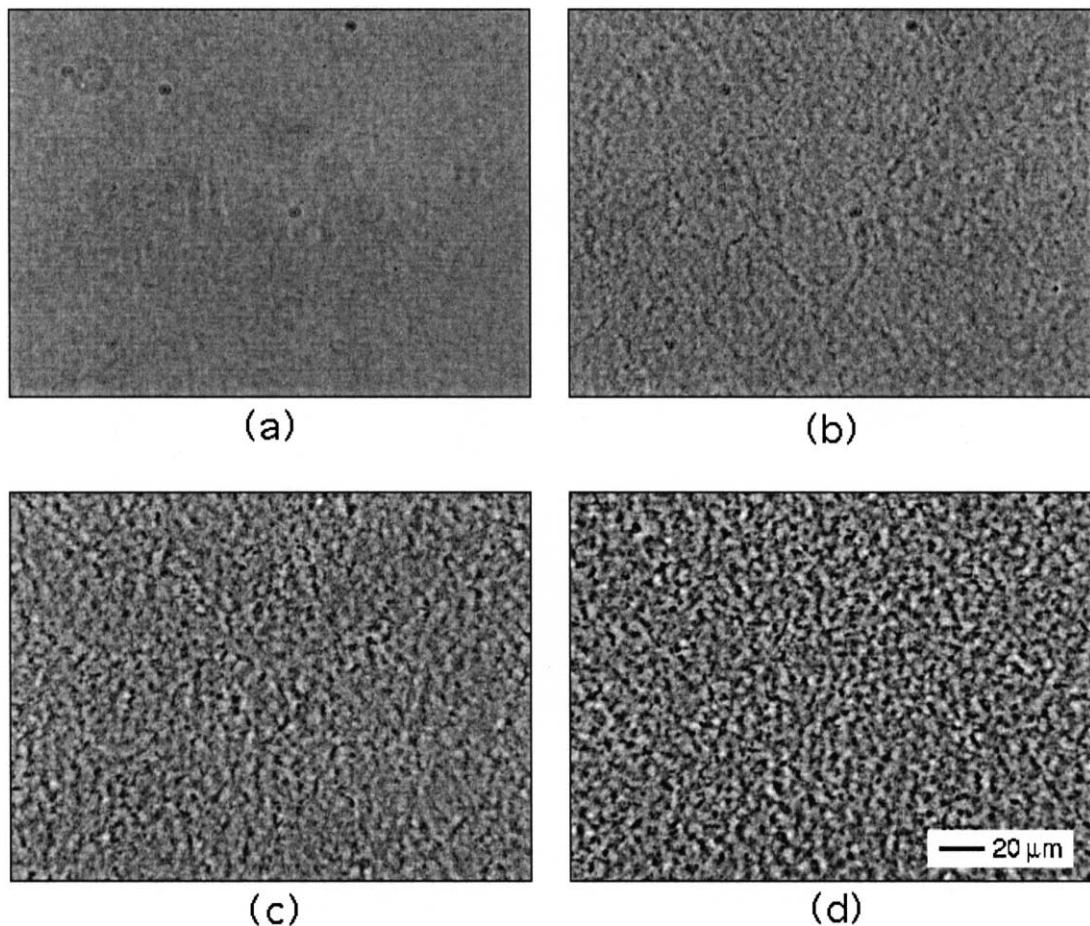


Fig. 6. Shear rate and shear time dependence of the contrast of shear-induced patterns. 2.5% WM in 0.5 N NaOH solution was sheared at 100 and 500 s<sup>-1</sup>. In (a), shear rate was 100 s<sup>-1</sup> and it did not show any time dependence. In (b)–(d), shear rate was 500 s<sup>-1</sup> and shear times were 1, 3, and 10 min, respectively. Time-dependent change in contrast is clearly shown.

Hence, the shear time dependence of pattern generation was studied at several fixed shear rates. To analyze the data quantitatively, the contrast factor of each pattern had to be calculated. The definition of contrast given in the text is

$$C = (I_{\max} - I_{\min})/(I_{\max} + I_{\min}) \quad (1)$$

where  $I$  stands for intensity of light in the image (Koenig, 1998). However, in the practical situation, the images contain a considerable amount of noise. In addition, since even illumination of the overall field of view is technically impossible, the light intensity of the captured images is not evenly distributed. In other words, the center part of the image is always brighter than the circumference.

To circumvent these problems, we generated a reference image file from each image by smoothing the image many times and subtracted it from the original image file. The sum of calculated numbers can be used as a measure of contrast. The newly defined contrast factor,  $\Delta$ , is

$$\Delta = \sum \sum \{I(i,j) - I_{\text{ref}}(i,j)\}^2 \quad (2)$$

Here,  $I(i,j)$  is the light intensity of the actual image at pixel

$(i,j)$  and  $I_{\text{ref}}(i,j)$  is that of the reference image. The intensity difference was squared to avoid canceling intensities by adding different signs. As the contrast of the image is increased, the numerical value of the contrast factor will be increased. The analysis result is shown in Fig. 7. From this analysis, it is clearly shown that the patterns are not formed below a certain critical shear rate. Also, the developing contrast of pattern increased faster with higher shear rate. Conclusively, we found two factors, higher shear rate and longer shear time, as required conditions for pattern formation.

Although the shear microscope data shows an overview of the formed patterns, the individual components of pattern-forming materials could not be identified. For clear visualization, the formed patterns were diluted with 0.2 N NaOH solution. With this technique, the individual particles that formed the pattern could be identified (Fig. 8). Their morphology reveals that pattern-forming materials are aggregates of molecules. Hence, the last question posed in Section 1 was answered.

As for the aggregation of starch molecules, the observed phenomena can be interpreted from two different points of view. The first viewpoint assumes that the aggregation is

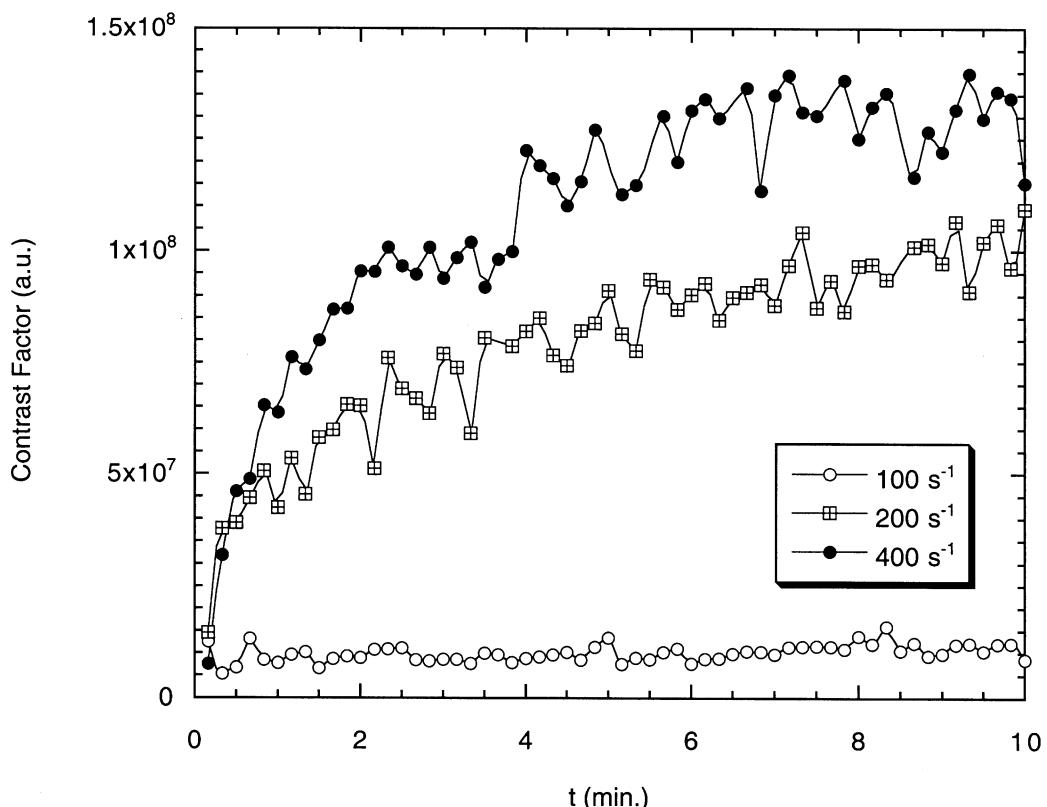


Fig. 7. The contrast variation of formed patterns shown as a function of time and shear rate. 2% WM in 0.2 N NaOH was used as a sample material. The definition of contrast factor is given in the text.

induced by the collision of solute particles in the shear field and the second one regards the pattern-forming materials as a product of shear-induced phase separation.

Swift and Friedlander adopted Smoluchowski's collision theory (Smoluchowski, 1917) to explain the coagulation of hydrosols in a simple shear field (Swift & Friedlander, 1964). The collision frequency between particles of radius  $r_i$  and  $r_j$  present at concentrations  $n_i$  and  $n_j$  is given by

$$f = (4S/3)(r_i + r_j)^3 n_i n_j \quad (3)$$

where  $S$  is the shear rate. According to this theory, the aforementioned two parameters taken as favorable conditions for pattern formation, high shear rate and long shear time, are justified. In addition, the theory predicts larger size particles as a favorable factor for aggregation. Actually, it is observed that incompletely solubilized starch solution forms a pattern more easily than well-solubilized solution. As a result of aggregation, the apparent molecular weight should have been increased causing lower solubility in the given solvent (Hiemenz, 1984). This would be the reason why starches are segregated from the solution after aggregation. The formed patterns disappear upon shaking. The binding force for aggregated molecules should be non-covalent, such as van der Waals force or hydrogen bonds because the formed pattern is not sturdy enough to withstand physical disturbances like shaking.

The second viewpoint explains the phenomenon with a concept of shear-induced phase separation. If this is the case, after shear-induced phase separation, the phase-separated starch molecules will be aggregated in the shear field. In the case of high molecular weight polystyrene in dioctylphthalate, the shift of the phase diagram by an applied shear field has been reported earlier (Hashimoto & Fujioka, 1991; Ver Strate & Phillipoff, 1974). Since the molecular weight of amylopectin is even higher than that of polystyrenes examined in those reports, it is not unreasonable to expect the same behavior with starch solutions. However, unlike polystyrene/dioctylphthalate solution, the formed pattern did not disappear upon removal of shear field in the case of starch solution. Although it looks stable, the formed patterns in starch solutions disappeared in a few days. If the slow disappearance of the formed pattern is just a matter of relaxation time, this second viewpoint still deserves to be investigated considering the extremely high molecular weight of amylopectin (Millard et al., 1999).

Both of the above viewpoints need to be verified with appropriate experiments. According to collision theory, the rate of aggregation by shear flow is independent of temperature. Hence the applicability of the theory to starch solutions can be verified by checking the temperature dependence of pattern formation. For the evaluation of the latter viewpoint, cloud point measurements as a function of applied shear field should be studied.

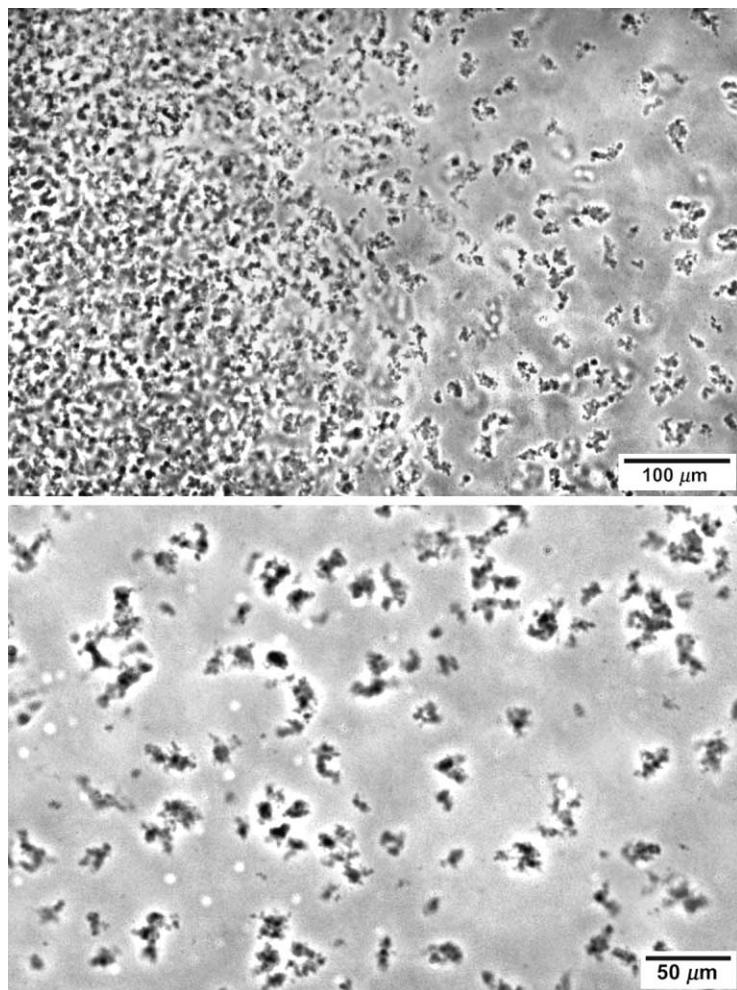


Fig. 8. Phase-contrast micrographs of 2% WM in 0.2 N NaOH solution sheared for 3 min at  $200\text{ s}^{-1}$ . To resolve individual particles, the sample was overlaid with 0.2 N NaOH before mounting the cover glass. The upper micrograph shows a continuum from confluent to individual particles observed at the edge of a dense region. The lower micrograph shows a higher magnification view of separate particles.

#### 4. Conclusions

Shear-thickening behavior and shear-induced pattern formation in semidilute starch solutions were studied in alkaline solution medium. Two instruments, a programmable rheometer and a shear microscope, were used for this study to clarify the processes occurring in these starch solutions.

It was found that gently prepared starch solutions are macroscopically heterogeneous with regions of highly concentrated starch clusters dispersed in relatively dilute starch solution. Under shear, starch from macroscopic regions of highly concentrated clusters would be dispersed into solution, raising the effective starch concentration and thus viscosity — that is, shear-thickening occurs. The shear-thickening is thus a result of breaking up of the highly concentrated gel-like starch clusters and resultant increase in effective starch concentration.

On the other hand, shear-induced pattern formation was shown to be the result of shear-induced aggregation. Direct observation using the shear microscope demonstrates that both shear rate and time are critical to this structure formation and it is independent of the shear-thickening phenomenon. Aggregates are formed above a certain critical shear rate and the extent of aggregation was increased as time.

For the mechanism of pattern formation, two viewpoints, collision theory and shear-induced phase separation, are suggested. The applicability of these theories to aggregation in starch solutions needs to be verified with further experiments.

#### Acknowledgements

The authors wish to thank Drs E.B. Bagley and F.R. Dintzis for their advice and fruitful discussions.

## References

- Dintzis, F. R., & Bagley, E. B. (1995). Shear-thickening and transient flow effects in starch solutions. *Journal of Applied Polymer Science*, 56, 637–640.
- Dintzis, F. R., Bagley, E. B., & Felker, F. C. (1995). Shear-thickening and flow-induced structure in a system of DMSO containing waxy maize starch. *Journal of Rheology*, 39, 1399–1409.
- Dintzis, F. R., Berhow, M. A., Bagley, E. B., Wu, Y. V., & Felker, F. C. (1996). Shear-thickening behavior and shear-induced structure in gently solubilized starches. *Cereal Chemistry*, 73, 638–643.
- Fishman, M. L., Rodriguez, L., & Chau, H. K. (1996). Molar masses and sizes of starches by high-performance size-exclusion chromatography with on-line multi-angle laser light scattering detection. *Journal of Agricultural and Food Chemistry*, 44, 3182–3188.
- Gallant, D. J., Bouchet, B., & Baldwin, P. M. (1997). Microscopy of starch: evidence of a new level of granule organization. *Carbohydrate Polymers*, 32, 177–191.
- Hashimoto, T., & Fujioka, K. (1991). Shear-enhanced concentration fluctuations in polymer solutions as observed by flow light scattering. *Journal of the Physical Society of Japan*, 60, 356–359.
- Hashimoto, T., & Kume, T. (1992). “Butterfly” light scattering pattern in shear-enhanced concentration fluctuations in polymer solutions and anomaly at high shear rates. *Journal of the Physical Society of Japan*, 61, 1839–1843.
- Hiemenz, P. C. (1984). *Polymer chemistry*, New York: Marcel Dekker (pp. 505–582).
- Kim, S., Yu, J.-W., & Han, C. C. (1996). Shear light scattering photometer with optical microscope for the study of polymer blends. *Review of Scientific Instruments*, 67, 3940–3947.
- Koenig, J. L. (1998). *Microscopic imaging of polymers*, Washington, DC: American Chemical Society (pp. 17–33).
- Millard, M. M., Wolf, W. J., Dintzis, F. R., & Willett, J. L. (1999). The hydrodynamic characterization of waxy maize amylopectin in 90% dimethyl sulfoxide–water by analytical ultracentrifugation, dynamic, and static light scattering. *Carbohydrate Polymers*, 39, 315–320.
- Moses, E., Kume, T., & Hashimoto, T. (1994). Shear microscopy of the “butterfly” pattern in polymer mixtures. *Physical Review Letters*, 72, 2037–2040.
- Smoluchowski, M.v. (1917). Versuch einer mathematischen Theorie der Koagulationskinetik kolloider Lösungen. *Z. Physik. Chem.*, 92, 129–168.
- Swift, D. L., & Friedlander, S. K. (1964). The coagulation of hydrosols by Brownian motion and laminar shear flow. *Journal of Colloid Science*, 19, 621–647.
- Ver Strate, G., & Philippoff, W. (1974). Phase separation in flowing polymer solutions. *Journal of Polymer Science Polymer Letters Edition*, 12, 267–275.